Theor Appl Climatol (2013) 111:149–160
DOI 10.1007/s00704-012-0650-x

ORIGINAL PAPER

# Spatiotemporal trends of aridity index in arid and semi-arid regions of Iran

**B. Shifteh Some'e · Azadeh Ezani · Hossein Tabari**

Received: 17 February 2012 / Accepted: 27 March 2012 / Published online: 27 April 2012


**Abstract** The spatiotemporal trends of aridity index in the arid and semi-arid regions of Iran in 1966–2005 were investigated using the Mann–Kendall test and Theil–Sen's slope estimator. The results of the analysis showed negative trends in annual aridity index at 55 % of the stations, while just one site had a statistically significant ($\alpha$=0.1) negative trend. Furthermore, the positive trends in the annual aridity index series were significant at the 95 % confidence level at Bushehr and Isfahan stations. The significant negative trend in the annual aridity index was obtained over Mashhad at the rate of −0.004. In the seasonal series, the negative trends in the spring and winter aridity index were larger compared with those in the other seasonal series. A noticeable decrease in the winter aridity index series was observed mostly in the southeast of the study area. In the summer and autumn aridity index, two significant positive trends were found.

## 1 Introduction

Continuously increasing levels of atmospheric carbon dioxide resulting in global warming, due to the increased greenhouse effect, are likely to have significant effects on the hydrological cycle (IPCC 2007). Greenhouse effect is a natural procedure that keeps the heat emitted from the earth's surface. According to the Intergovernmental Panel on Climate Change (IPCC 2007), the three main reasons of the increase in greenhouse gases observed over the past two centuries have been fossil fuels, land use, and agriculture. The consequence is that greenhouse effect is becoming stronger, and as a result, the earth is becoming warmer. Over the last century, the average of the Earth's surface air temperature has risen by a little less than 1°C. Moreover, according to the IPCC (2007), the global surface temperature will probably rise a further 1.1–6.4°C in the twenty-first century. The warming has also not been geographically uniform, and the rate of warming in some part of the world such as southwest Asia was found to be slightly higher than for the global land areas in general (Hulme 1996). Climate change will implicate indeterminate changes in seasonal patterns of temperature, precipitation, air humidity, snow cover, and frequency and severity of extreme events (Le Houérou 1996).

Developing countries (such as Iran) are the most vulnerable to climate change impacts because they have fewer resources to adapt socially, technologically, and economically. Furthermore, it is predicted that arid and semi-arid areas will receive even less rain under climate change, leading to the degradation of agricultural land and impacting food security (UNFCCC 2007). A more arid climate is usually accompanied by an increase in the frequency and severity of droughts (Heathcote 1986). As a result, a more proactive approach to drought planning and water crisis management is needed, and it becomes increasingly more urgent before a drought or water crisis affects water resources. Land degradation is a serious problem that crosses national borders, ecological zones, and socioeconomic levels, and it can be especially devastating for the world's

B. Shifteh Some'e (✉) · A. Ezani
Department of Water Engineering, Ardabil Branch,
Islamic Azad University,
Ardabil, Iran
e-mail: b.shifteh.s@gmail.com

A. Ezani
e-mail: ezani.azadeh@gmail.com

H. Tabari
Department of Water Engineering, Ayatollah Amoli Branch,
Islamic Azad University,
Amol, Iran
e-mail: tabari.ho@gmail.com

poorest people living in dryland areas (FAO 2008). Many countries are located in drylands in which the water resources are limited (Tabari et al. 2011a) and degradation places the regions in serious risk of desertification. Iran is one of the most arid countries of the world, with more than 75 % of its area having been classified as arid or semi-arid.

The one binding factor to all arid areas is aridity. Aridity is usually expressed as a function of rainfall and temperature. A useful description of aridity is the following climatic aridity index ($P$/PET). Aridity results from the presence of dry, descending air. Therefore, aridity is found mostly in places where anticyclonic conditions are persistent, as is the case in the regions lying under the anticyclones of the subtropics. Few previous studies focused on aridity issues throughout the world (Ben-Gai et al. 1994; Turkes 1999; Zhang et al. 2009; Onder et al. 2009; Golian et al. 2010; Kousari et al. 2011). Turkes (2003) analyzed the annual and seasonal precipitation series and annual aridity index series of Turkey in 1930–1993. He found a general tendency from humid conditions of around 1960s toward dry sub-humid climatic conditions in the aridity index values of many stations of Turkey. Wu et al. (2006) studied the general moisture conditions and the annual and seasonal trends of temperature, precipitation, potential evapotranspiration, and aridity index from 1971 to 2000 in China. The results showed increasing trends in surface air temperature and precipitation and decreasing trends in potential evapotranspiration and aridity index. Rai et al. (2010) reported an overall falling trend in annual rainfall, monsoon rainfall, annual rainy days, monsoon rainy days, and aridity index over the Yamuna River Basin of India.

Karimi Kakhk and Sepehri (2011) investigated climate change at Hamedan and Tabriz stations in Iran during two periods of 55 and 41 years ending in 2005. Their results showed that the aridity index had a downward trend in consequence of precipitation decrease and evapotranspiration increase at Tabriz station that led to a rise in climate aridity. Ghasemi et al. (2008) modeled mean long-term climatic data through Shuttle Radar Topographic Mission 90m digital elevation model in GIS software for the delineation of agro-climate zoning units. Their results showed that based on UNESCO's method, areas with aridity indices higher than 0.5 are classified as sub-humid, humid, and ultra-humid zones, capable of being used in normal agriculture, whereas areas with aridity indices higher than 0.65 are mostly located on highlands with temperature and length of growing period limitations and normally covered by forests. Tabari and Aghajanloo (2012) analyzed monthly and annual aridity index, utilizing the ratio of precipitation over reference evapotranspiration, at ten stations located in the north and northwest regions in Iran using the Kendall and Spearman tests. They found an increase in aridity during the study period (1966–2005), and the increase was more obvious in the semi-arid region (Northwest Iran) than in the humid region (North Iran). The increase of aridity was caused by the concurrent occurrences of negative precipitation trends and positive reference evapotranspiration trends.

In this research, we present a study of aridity index in the arid and semi-arid regions of Iran for the period 1966–2005 using the Mann–Kendall test and Theil–Sen's slope estimator. Based on meteorological data from 22 synoptic stations, we initially calculated the annual and seasonal aridity index, $P/\mathrm{ET_o}$ (where $P$ is precipitation and $\mathrm{ET_o}$ is the reference evapotranspiration) and then applied the tests to the time series. Moreover, the serial correlation effects on the Mann–Kendall test and Sen's slope estimator were evaluated.

## 2 Materials and methods

### 2.1 Data and methodology

Examination of climate changes needs long and high-quality records of climatic variables. Therefore, the time series of records from 22 meteorological synoptic stations including maximum ($T_{max}$), minimum ($T_{min}$), and mean air temperature ($T_{mean}$); wind speed ($U$); relative humidity (RH); sunshine hours ($n$); vapor pressure ($e_a$); and precipitation ($P$) from 1st January 1966 to 31st December 2005 were collected for this study from the Islamic Republic of Iran Meteorological Organization. Spatial distributions of the stations are shown in Fig. 1. In addition, details of the synoptic stations and their data availability are presented in Table 1.

Data collection and measurements are in many cases associated with some uncertainties due to measurement errors and other known and unknown factors, including missing data. Hence, first of all, data were quality-controlled with the double-mass curve analysis (Kohler 1949). The solar radiation gaps were also filled using the Angstrom equation (Allen et al. 1998).

$$R_s = \left(a_s + b_s \frac{n}{N}\right) R_a \tag{1}$$

where $R_s$ is the solar radiation (in megajoules per square meter per day), $R_a$ is the extraterrestrial radiation (in megajoules per square meter per day), $n$ is the actual duration of sunshine (hours), $N$ is the maximum possible duration of sunshine or daylight hours (hours), $a_s$ is the regression constant expressing the fraction of extraterrestrial radiation reaching the earth on overcast days ($n$=0), and $a_s + b_s$ is the

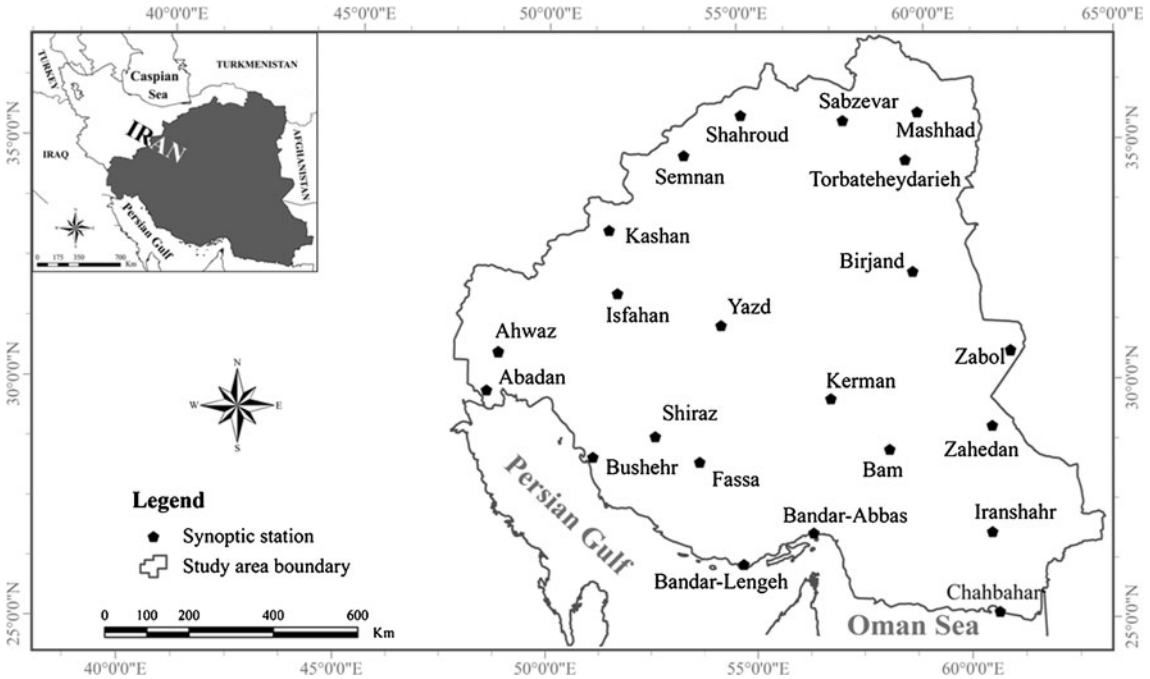


**Fig. 1** Spatial distribution of the synoptic stations in the study area

fraction of extraterrestrial radiation reaching the earth on clear days ($n=N$). Where sunshine data are lacking, Hargreave's radiation formula (Hargreaves and Samani 1985) was used to estimate solar radiation.

**Table 1** Geographic and climatic characteristics and data availability of the synoptic stations used in the study

| Station | Longitude (E) | Latitude (N) | Elevation (m a.s.l) | Data availability (%) | Climate type (De Martonne 1926)[a] |
|---|---|---|---|---|---|
| 1. Abadan | 52°40′ | 31°11′ | 2,030 | 99.7 | Arid |
| 2. Ahwaz | 48°40′ | 31°20′ | 23 | 100 | Arid |
| 3. Bam | 58°21′ | 29°06′ | 1,067 | 100 | Arid |
| 4. Bandar-Abbas | 56°22′ | 27°13′ | 10 | 100 | Arid |
| 5. Bandar-Lengeh | 54°50′ | 26°32′ | 23 | 99.5 | Arid |
| 6. Bushehr | 50°50′ | 28°59′ | 20 | 100 | Arid |
| 7. Birjand | 59°12′ | 32°52′ | 1,491 | 99.5 | Arid |
| 8. Chahbahar | 60°37 | 25°17′ | 8 | 91.8 | Arid |
| 9. Fassa | 53°41′ | 28°58′ | 1,288 | 100 | Semi-arid |
| 10. Iranshahr | 60°42′ | 27°12′ | 591 | 100 | Arid |
| 11. Isfahan | 51°40′ | 32°37′ | 1,550 | 96.8 | Arid |
| 12. Kashan | 51°27′ | 33°59′ | 982 | 100 | Arid |
| 13. Kerman | 56°58′ | 30°15′ | 1,754 | 99.5 | Arid |
| 14. Mashhad | 59°38′ | 36°16′ | 999 | 100 | Semi-arid |
| 15. Shiraz | 52°36′ | 29°32′ | 1,484 | 100 | Semi-arid |
| 16. Sabzevar | 57°43′ | 36°12′ | 978 | 100 | Arid |
| 17. Semnan | 53°33′ | 35°35′ | 1,131 | 100 | Arid |
| 18. Shahroud | 54°57′ | 36°25′ | 1,345 | 100 | Arid |
| 19. Torbateheydarieh | 59°13′ | 35°16′ | 1,451 | 100 | Semi-arid |
| 20. Yazd | 54°17′ | 31°54′ | 1,237 | 99.3 | Arid |
| 21. Zabol | 61°29′ | 31°02′ | 489 | 100 | Arid |
| 22. Zahedan | 60°53′ | 29°28′ | 1,370 | 100 | Arid |

[a]Tabari et al. (2011a)

### 2.2 Estimation of aridity index

UNESCO (1979) applied an aridity/humidity classification system based on the average annual precipitation divided by the average annual potential evapotranspiration (PET). According to UNESCO (1979), PET is calculated using Penman's (1948) equation. Later, UNEP (1992) proposed to estimate PET using the simple Thornthwaite (1948) formula that requires only air temperature data. The index proposed by UNEP is widely known as the aridity index, which is also used by FAO. In addition, the index was utilized as the agro-climatological index, incorporating climatological specifications as well as crop moisture needs (Sadeghi et al. 2002).

Jensen et al. (1990) proposed the term "reference evapotranspiration" instead of PET to underline its meaning. Following Paltineanu et al. (2007) and Khalili et al. (2011), the $ET_o$ values calculated by the Thornthwaite ($ET_{o\text{-}TH}$) and Penman ($ET_{o\text{-}P}$) equations were replaced with the $ET_o$ values of the Penman–Montieth FAO 56 method ($ET_{o\text{-}PMF\text{-}56}$). Use of $ET_{o\text{-}PMF\text{-}56}$ rather than $ET_{o\text{-}TH}$ and $ET_{o\text{-}P}$ was recommended by Jensen et al. (1990) and Allen et al. (1998). It should be noted that the considered stations are the official sites with complete weather data as required by the Penman–Montieth FAO 56 method.

The Penman–Monteith method assumes the $ET_o$ as that from a hypothetical crop with an assumed crop height (0.12 m) and a fixed canopy resistance (70 $Sm^{-1}$) and albedo (0.23), closely resembling the evapotranspiration from an extensive surface of green grass cover of uniform height, actively growing, and not short of water, which is given by Allen et al. (1998) as follows:

$$ET_o = \frac{0.408\Delta(R_n - G) + \gamma \frac{900}{T_{mean}+273} U_2(e_s - e_a)}{\Delta + \gamma(1 + 0.34U_2)} \quad (2)$$

where $ET_o$ is the reference evapotranspiration (in millimeters per day), $R_n$ is the net radiation (in megajoules per square meter per day), $G$ is the soil heat flux (in megajoules per square meter per day), $\gamma$ is the psychometric constant (in kilopascals per degree Celsius), $e_s$ is the saturation vapor pressure (in kilopascals), $e_a$ is the actual vapor pressure (in kilopascals), $\Delta$ is the slope of the saturation vapor pressure–temperature curve (in kilopascals per degree Celsius), $T_{mean}$ is the average daily air temperature (degree Celsius), and $U_2$ is the mean daily wind speed at 2 m (in meters per second). The computation of all data required for calculating $ET_o$ followed the method and procedure given in Chapter 3 of FAO-56 (Allen et al. 1998).

### 2.3 Statistical tests for trend analysis

One of the most principal requirements of research about climate change is to analyze and discover historical changes in the climatic parameters. In recent years, many studies were carried out to the historical analysis of climatic variables trend throughout the world such as temperature (e.g., Yue and Hashino 2003; Gadgil and Dhorde 2005; Rebetez and Reinhards 2008; Choi et al. 2009; Tabari and Hosseinzadeh Talaee 2011a, 2011b; El Kenawy et al. 2011; Tabari et al. 2012b; del Río et al. 2011; Croitoru et al. 2012), precipitation (e.g., Buffoni et al. 1999; Cannarozzo et al. 2006; Partal and Kahya 2006; Liu et al. 2008; Kampata et al. 2008; Tabari and Hosseinzadeh Talaee 2011c; Tabari et al. 2012a, 2011e), evaporation (e.g., Jhajharia et al. 2009; Tabari and Marofi 2011), and evapotranspiration (e.g., Liang et al. 2010; Espadafor et al. 2011; Eslamian et al. 2011; Tabari et al. 2011a, c, 2012c).

#### *2.3.1 Mann–Kendall test*

The Mann–Kendall (MK) test is one of the most important statistical methods commonly used for detecting a trend in hydroclimatic time series. The MK test is a simple and robust method and can cope with missing values and values below a detection limit. In addition, the test is suitable for data that do not follow a normal distribution (Tabari et al. 2011b, 2012d). The MK test is given as:

$$S = \sum_{k=1}^{n-1} \sum_{j=k+1}^{n} \operatorname{sign}(x_j - x_k) \quad (3)$$

$$\operatorname{sign}(x_j - x_k) = \operatorname{sign}(R_j - R_i) = \begin{cases} +1 & \text{if } (x_j - x_k) \succ 0 \\ 0 & \text{if } (x_j - x_k) = 0 \\ -1 & \text{if } (x_j - x_k) \prec 0 \end{cases} \quad (4)$$

$$\operatorname{Var}(S) = \frac{[n(n-1)(2n+5)] - \sum_{i=1}^{m} t_i(t_i-1)(2t_i+5)}{18} \quad (5)$$

where $n$ is the number of data points, $t_i$ is the number of ties for the $i$ value, and $m$ is the number of tied values. Then, Eqs. 3 and 4 were used to compute the test statistic $Z$ from the following equation:

$$Z = \begin{cases} \dfrac{S-1}{\sqrt{\operatorname{Var}(S)}} & \text{if} \quad S \succ 0 \\ 0 & \text{if} \quad S = 0 \\ \dfrac{S-1}{\sqrt{\operatorname{Var}(S)}} & \text{if} \quad S \prec 0 \end{cases} \quad (6)$$

A positive value of $Z$ indicates that there is an increasing trend, and a negative value indicates a decreasing trend. The null hypothesis, $H_0$, that there is no trend in the records is either accepted or rejected depending on whether the computed $Z$ statistics is less than or more than the critical value of $Z$ statistics obtained from the normal distribution table at the 5 % significance level (Kampata et al. 2008).

*2.3.2 Theil–Sen's estimator*

The slope of $n$ pairs of data points was estimated using Theil–Sen's estimator (Sen 1968; Theil 1950), which is given by Eq. 7:

$$\beta = \text{Median}\left(\frac{x_i - x_j}{t_i - t_j}\right) \tag{7}$$

where $x_i$ and $x_j$ are data values at times $t_i$ and $t_j$ ($i>j$), respectively.

According to Yue et al. (2002), the slope calculated by Theil–Sen's estimator is a robust estimate of the magnitude of a trend, which has been widely used in identifying the slope of the trend line in hydrological time series (e.g., Dinpashoh et al. 2011; Mohsin and Gough 2009).

## 2.4 Serial correlation on the Mann–Kendall test

The Mann–Kendall test requires a time series to be serially independent (Yue and Wang 2002). According to Cox and Stuart (1955), a positive serial correlation between the observations would increase the chance of significant answer, even in the absence of a trend. The effect of serial correlation can be eliminated by removing serial correlation from the time series before applying trend tests or by modifying the original trend test to account for serial correlation (Hamed 2008). The pre-whitening method was proposed by von Storch and Navarra (1995) to eliminate the influence of lag-1 serial correlation on the MK test, but the method will remove a portion of the detected trend and change the MK test results (Wu et al. 2008). Yue et al. (2002) modified the pre-whitening method as trend-free pre-whitening (TFPW) to the series in which there was a significant serial correlation. The TFPW procedure can be represented as follows:

$$Y_i = x_i - (\beta \times i) \tag{8}$$

where $\beta$ is Theil–Sen's estimator (Eq. 7). The lag-1 serial correlation coefficient ($r_1$) of the new series is calculated. If $r_1$ is not significantly different from zero, the sample data are considered to be serially independent and the MK test is directly applied to the original sample data. Otherwise, it is considered to be serially correlated, and pre-whitening is used before applying the MK test as follows:

$$Y_i^{'} = Y_i - r_1 \times Y_{i-1} \tag{9}$$

Then, the value of $\beta \times i$ is added again to the residual data set of Eq. 9 as

$$Y_i^{''} = Y_i^{'} + (\beta \times i) \tag{10}$$

The $Y''_i$ series is the final (or pre-whitened) series.

The TFPW method has been applied in many of the recent studies to detect trends in hydrological and meteorological parameters (e.g., Yue et al. 2002, 2003; Aziz and Burn 2006; Novotny and Stefan 2007; Wu et al. 2008; Kumar et al. 2009; Dinpashoh et al. 2011; Tabari et al. 2012a, b).

## 2.5 Relative change

To compute the relative change of the annual and seasonal aridity indices, the following equation was used:

$$\text{RC} = \frac{n \times \beta}{|x|} \times 100 \tag{11}$$

where $n$ is the length of trend period (years), $\beta$ is the magnitude of the trend slope of the time series which is determined by Sen's median estimator, and $|x|$ is the absolute average value of the time series.

In this work, contours for trend maps were generated using an inverse distance-weighted algorithm with a power of 2.0 for each grid point, and data from locations within a 290-km radius were used. For these operations, the ArcGIS 9.3 software was used.

# 3 Results and discussion

## 3.1 Spatial distribution of the mean annual and seasonal aridity index

Figure 2 shows the spatial distribution of the long-term mean annual and seasonal aridity index ($P/\text{ET}_o$) in the study area. The distribution of the annual and seasonal $P/\text{ET}_o$ revealed strong gradients, with higher values corresponding to the south of the analyzed area located in the north of the Persian Gulf and Oman Sea and the lower values obtained in the central part of the region toward the north. The southeast region of Iran is extremely arid, and its main feature is local winds, called "120-day Sistan winds," that blow, primarily, in summer hot months. In addition, the ground mainly is bare, and very sparse desert vegetation may be found in some parts of the region (Dinpashoh 2006).

The mean annual (summer) $P/\text{ET}_o$ of the study area varied between 0.06 (0.0001) at Zabol station and 7.04 (11.13) at Abadan station. The spatial pattern of the $P/\text{ET}_o$ variations is similar to that of the $\text{ET}_o$ variations found by Tabari et al. (2011a).

## 3.2 Annual trends of aridity index

The results of the MK test for the annual trends of aridity index data are shown in Fig. 3a. Both positive and negative

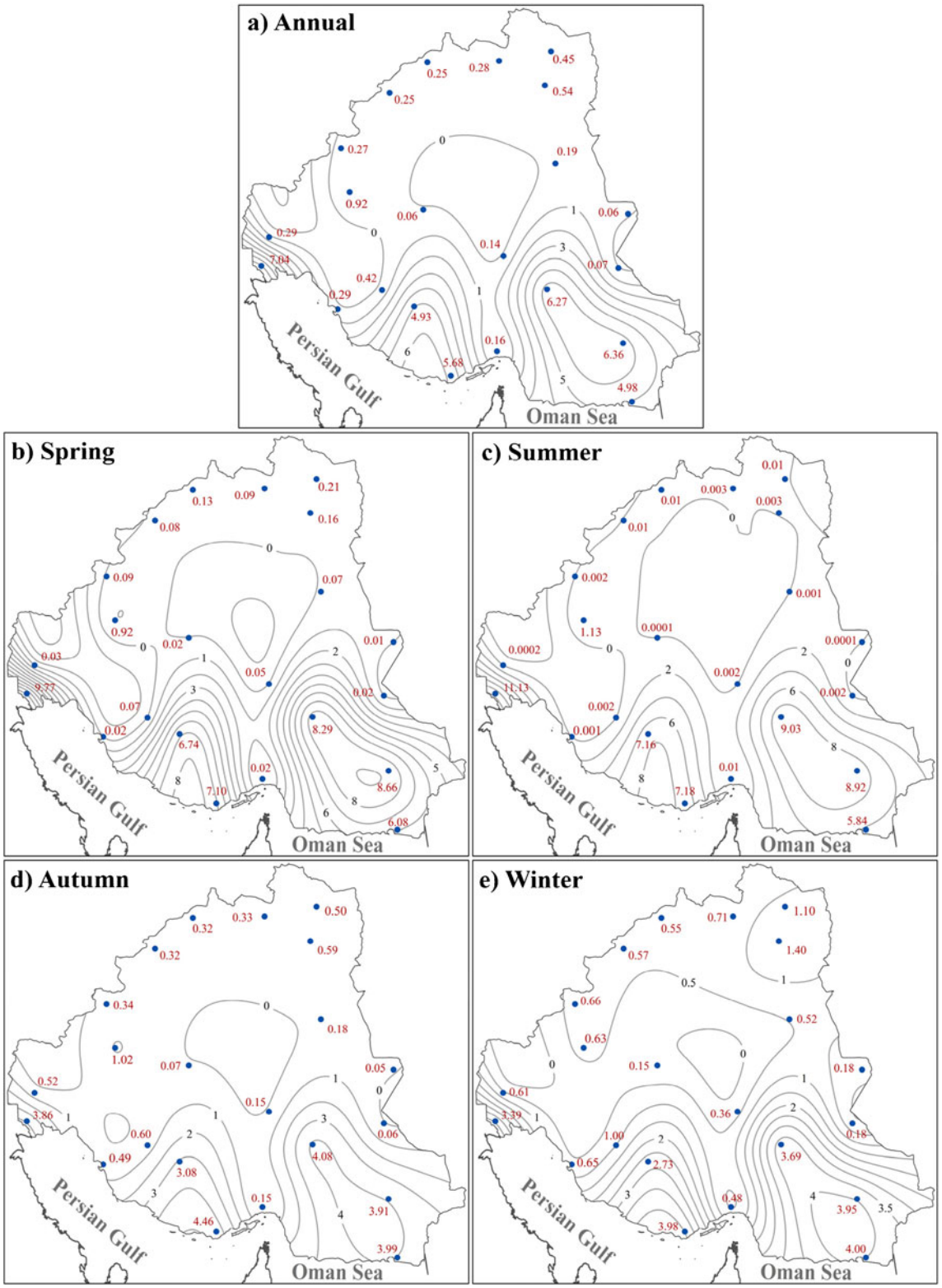


**Fig. 2** Spatial distribution of annual and seasonal aridity index in the study area

trends were identified by the MK test in annual $P/ET_o$ data. Nevertheless, most of the trends were insignificant at the 90 and 95 % confidence levels. Decreasing trends in annual $P/ET_o$ were observed in 55 % of the stations with the Mann–Kendall test. The decreasing trends were significant ($\alpha$=0.1) at Mashhad station in the northeast of the study area. The

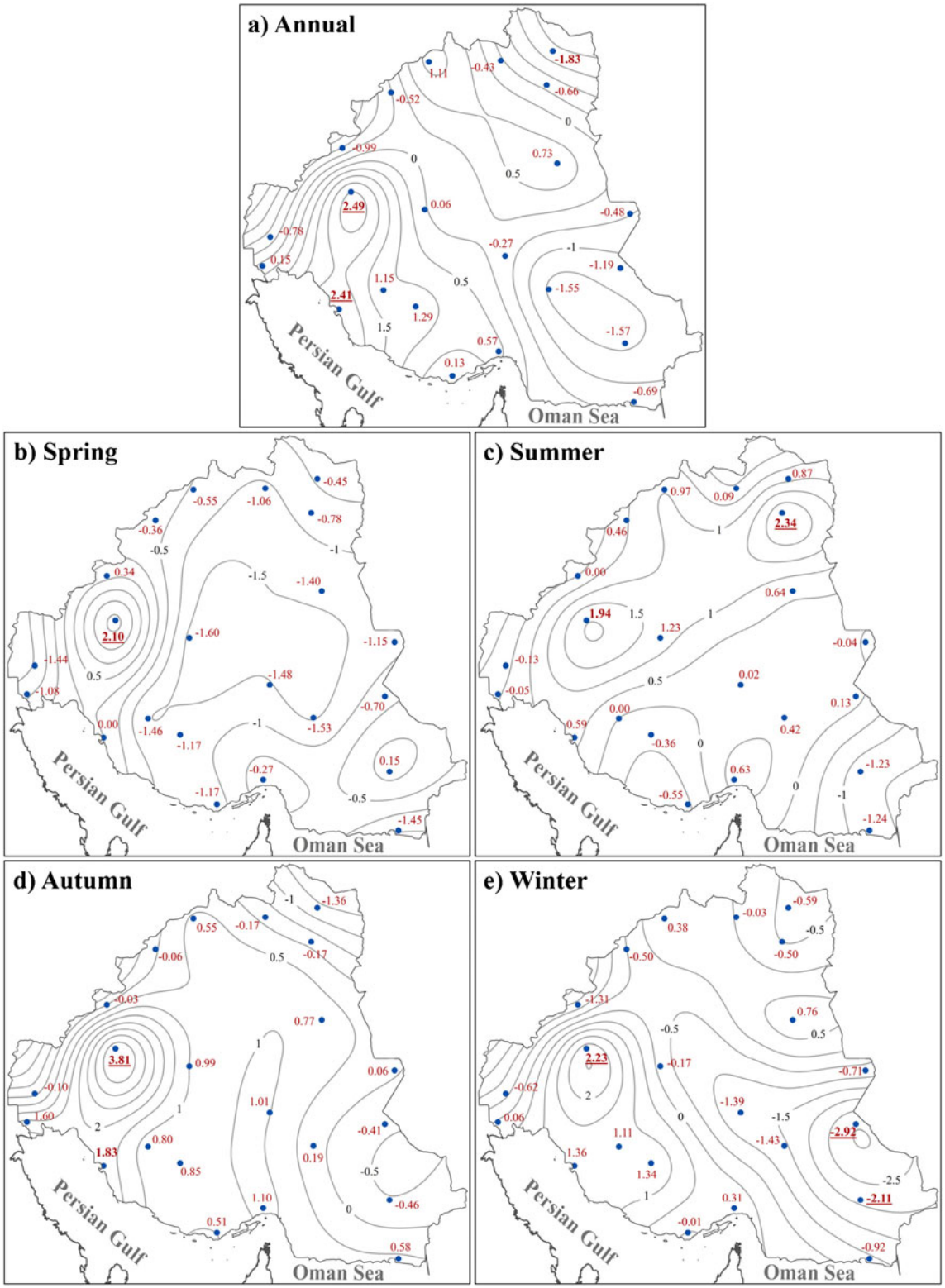


**Fig. 3** Spatial distribution of the statistics *Z* of the Mann–Kendall test for the annual and seasonal aridity index (1966–2005). (*Bold* and *bold underlined* values indicate significant correlations at the 90 and 95 % confidence levels, respectively)

decreased aridity in Mashhad station is mainly due to the significant increasing trend of reference evapotranspiration (Tabari et al. 2011a). The significant negative trend in annual aridity index was found over Mashhad at the rate of −0.004. Furthermore, the positive trends in the annual aridity index series were found to be significant at the 95 %

confidence level at Bushehr and Isfahan stations (Fig. 3a). The significant increasing $P$ trend (Tabari and Hosseinzadeh Talaee 2011c) and significant decreasing $ET_o$ trend (Tabari et al. 2011c) at Bushehr station were responsible for the increased aridity at that station. Similarly, the increased aridity at Isfahan station was attributed to significant decreasing $ET_o$ trend (Tabari et al. 2011a) and insignificant increasing $P$ trend (Tabari and Hosseinzadeh Talaee 2011c).

In addition, the strongest significant positive trends in annual $P/ET_o$ were observed at the rates of +0.002 and +0.004, respectively. The graph of time series and linear trends of annual aridity index at the stations with significant trends are presented in Fig. 4. The relative change of the annual aridity index is presented in Fig. 5a, showing that the annual aridity index decreased from 10 % to more than 30 % in the northeast and southeast parts. There are some exceptions, like central regions and some other parts of Iran. Adversely, the results for the most stations located on the coastal areas of the Persian Gulf indicated positive trends.

### 3.3 Seasonal trends of aridity index

For all the stations in the study area, the MK test was also applied to detect the temporal trends of the seasonal $P/ET_o$ time series (Fig. 3b–e). The majority of the trends in the spring $P/ET_o$ time series were negative, accounting for about 82 % of the trends (Fig. 3b). Based on the results of the MK test, the significant negative trends at the 95 % confidence level in the spring $P/ET_o$ series were found at Iranshahr and Zahedan stations (Fig. 3b). In contrast, the significant positive trends at the 95 % confidence level in the spring $P/ET_o$ series were found at Isfahan station (Fig. 3b). Spring $P/ET_o$ at almost all parts of the study area decreased by more than 30 % and increased in the northwest and southeast parts by exceeding 10 % (Fig. 5b). Around 77 and 55 % of the monthly aridity index series respectively in the northwest and north regions of Iran were also characterized by a decreasing trend (Tabari and Aghajanloo 2012).

In summer $P/ET_o$, significant trends were found only at Isfahan and Torbatheydarieh stations, and they were positive. In summer, excluding the north and the northwest parts of the study area, $P/ET_o$ decreased by 10 % or more (Fig. 5c). The autumn $P/ET_o$ series demonstrated negative trends at 36 % of the stations, but none of them were statistically significant. Among the positive trends, significant trends at the 90 and 95 % confidence levels were found at Bushehr and Isfahan stations, respectively. Autumn $P/ET_o$ mainly decreased in the northeast part by more than 30 %, while increases were confined to the central parts toward the southwest regions by 30 % or more (Fig. 5d). The increased aridity will enhance future risk and vulnerability of crop production related to water availability, especially during the growing season. Rainfed agriculture is affected more directly by aridity than irrigated agriculture. Therefore, as a result of aridity increase in the region, yield performance of rainfed agriculture will exhibit more volatility.

Similar to the spring and summer series, most of the trends in the winter $P/ET_o$ time series were negative, accounting for about 64 % of the stations (Fig. 5e). Nevertheless, the significant negative trends in winter $P/ET_o$ were larger compared with those in the other seasonal series. Two significant negative trends were detected in the winter time series at Iranshahr and Zahedan stations which are located in the southeast part of the region (Fig. 5e).

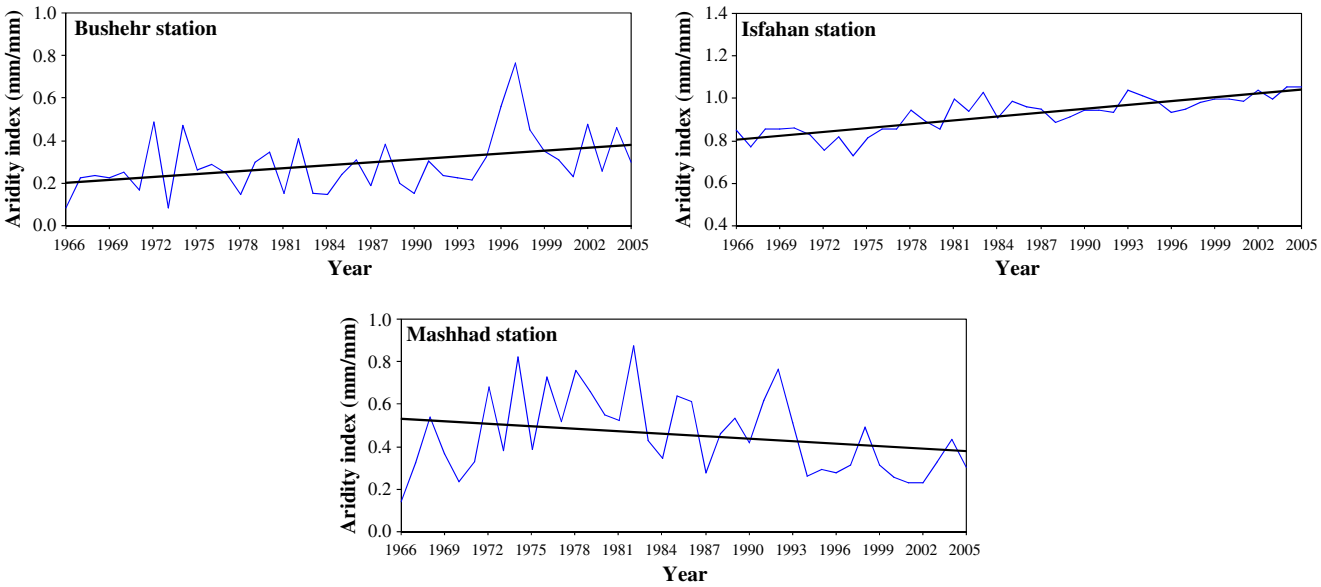


**Fig. 4** Graph of time series and linear trends of annual aridity index at the stations with the significant trends

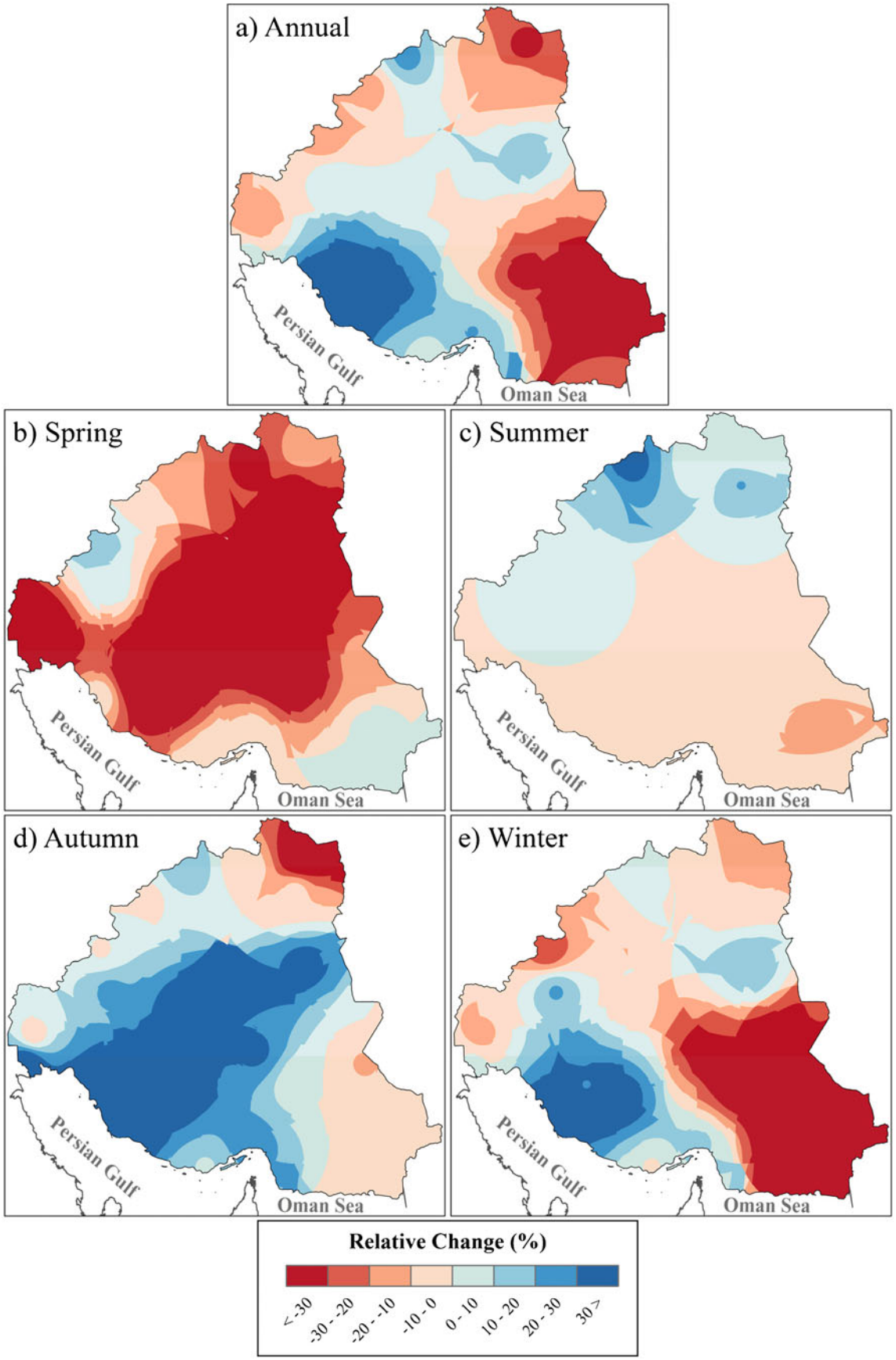


**Fig. 5** Relative change for the annual and seasonal aridity index in 1966–2005

While winter $P/ET_o$ in the southeast parts (north of the Oman Sea) decreased by more than 30 %, it increased at the southwest part (north of the Persian Gulf) by exceeding 30 %. Furthermore, the pattern of the winter $P/ET_o$ trends was extremely similar to the annual one, which shows the great role of winter $P/ET_o$ in annual $P/ET_o$. Any increase in aridity level in the study area with severe consequences of water scarcity may have serious effects on the agriculture and economy of the country.

Significant negative trends in seasonal $P/ET_o$ ranged between −0.004 at Zahedan station and −0.11 at Iranshahr station in winter. In addition, the highest significant increase of $P/ET_o$ values was obtained in autumn data over Bushehr at the rate of +0.007. Tabari and Aghajanloo (2012) found that the north and northwest regions of Iran have become more arid over the last 40 years. They reported that the increased aridity was associated with the concurrent occurrences of the decreasing P trends and the increasing $ET_o$ trends. In Turkey, Onder et al. (2009) evaluated changes in aridity by comparing the current and future index values. They showed an increase in aridity for 2070s over the whole country, except the northeastern part. In addition, there has been a general tendency from humid conditions of around the 1960s toward dry sub-humid climatic conditions in Turkey (Turkes 1999).

## 4 Conclusions

In this paper, the Mann–Kendall trend test and Theil–Sen's slope estimator were used to investigate the spatiotemporal trends and variability of $P/ET_o$ data from 22 synoptic stations in Iran on the annual and seasonal timescales for the period 1966–2005. Over the 40-year period, a negative trend in annual $P/ET_o$ occurred at 12 sites (55 %), while only one site had a statistically significant ($\alpha$=0.1) negative trend in $P/ET_o$. Adversely, the positive trends in the annual aridity index series were significant at the 95 % confidence level at Bushehr and Isfahan stations. The magnitude of the significant negative trends in annual $P/ET_o$ at Mashhad station was −0.004. In addition, the highest and lowest rates of significant positive trends in annual $P/ET_o$ were found to be +0.002 and +0.004, respectively. The spatial distribution of the annual $P/ET_o$ trends indicated that the negative trends mostly happened in the northeast and southeast parts of the region, which decreased by 10 % to more than 30 %. Adversely, most of the stations situated in the north of the Persian Gulf coastal areas showed positive trends.

Analysis of the seasonal $P/ET_o$ series showed a mix of negative and positive trends. However, the negative trends in the spring and winter $P/ET_o$ series were larger compared with those in the other seasonal series so that two significant negative trends were detected in the winter time series. Winter $P/ET_o$ has been noticed as having negative trends in the southeast parts of the study regions. In summer and autumn $P/ET_o$, two significant positive trends were detected by the trend tests.

Information regarding changes in the $P/ET_o$ index as a result of climate change is necessary for policy makers and managers within the context of water resources management, hydrology, agriculture, and environment. Consequently, it indicates the need for more concentration to climate change and different aspects of its effect in the $P/ET_o$ regime of a given region. All these findings can help provide reasonable managerial strategy in relation to water resources management. Nonetheless, more studies are needed in the areas to prove the magnitude, effect, and risks on the ecosystems.

**Acknowledgment** We thank the Islamic Republic of Iran Meteorological Organization (IRIMO) for providing the required climatic data of the various stations. We also thank the two anonymous reviewers for their constructive criticism and helpful comments.

## References

Allen RG, Pereira LS, Raes D, Smith M (1998) Crop evapotranspiration. guidelines for computing crop water requirements. Irrig Drain Paper 56, FAO, Rome

Aziz OIA, Burn DH (2006) Trends and variability in the hydrological regime of the Mackenzie River Basin. J Hydrol 319(1–4):282–294

Ben-Gai T, Bitan A, Manes A, Alpert P (1994) Long-term changes in annual rainfall patterns in southern Israel. Theor Appl Climatol 49 (2):59–67

Buffoni L, Maugeri M, Nanni T (1999) Precipitation in Italy from 1833 to 1996. Theor Appl Climatol 63:33–40

Cannarozzo M, Noto LV, Viola F (2006) Spatial distribution of rainfall trends in Sicily (1921–2000). Phys Chem Earth 31(18):1201–1211

Choi G, Collins D, Ren G, Trewin B, Baldi M, Fukuda Y, Afzaal M, Pianmana T, Gomboluudev P, Huong PTT, Lias N, Kwon W-T, Boo K-O, Cha Y-M, Ya Z (2009) Changes in means and extreme events of temperature and precipitation in the Asia-Pacific Network region, 1955–2007. Int J Climatol 29:1906–1925

Cox DR, Stuart A (1955) Some quick sign tests for trend in location and dispersion. Biometrika 42:80–95

Croitoru AE, Holobaca IH, Lazar C, Moldovan F, Imbroane A (2012) Air temperature trend and the impact on winter wheat phenology in Romania. Clim Chang 111:393–410

del Río S, Herrero L, Pinto-Gomes C, Penas A (2011) Spatial analysis of mean temperature trends in Spain over the period 1961–2006. Glob Planet Chang 78:65–75

Dinpashoh Y (2006) Study of reference crop evapotranspiration in I.R. of Iran. Agric Water Manag 84:123–129

Dinpashoh Y, Jhajharia D, Fakheri-Fard A, Singh VP, Kahya E (2011) Trends in reference crop evapotranspiration over Iran. J Hydrol 399:422–433

El Kenawy A, Lopez-Moreno JI, Vicente-Serrano SM (2011) Recent trends in daily temperature extremes over northeastern Spain. Nat Hazards Earth Syst Sci 11:2583–2603

Eslamian S, Khordadi MJ, Abedi-Koupai J (2011) Effects of variations in climatic parameters on evapotranspiration in the arid and semi-arid regions. Glob Planet Chang 78:188–194

Espadafor M, Lorite IJ, Gavlian P, Berengena J (2011) An analysis of the tendency of reference evapotranspiration estimates and other climate variables during the last 45 years in Southern Spain. Agric Water Manag 98:1045–1061

FAO (2008) Land Degradation Assessment in Drylands (LADA), assessing the status, causes and impact of land degradation. Food and Agriculture Organization of the United Nations, Rome

Gadgil A, Dhorde A (2005) Temperature trends in twentieth century at Pune, India. Atmos Environ 35:6550–6556

Ghasemi VR, Mahmoudi S, Ghafari AAA, de Pauw E (2008) Agro-climate zoning (ACZ) through UNESCO approach and modified aridity index in some parts of East Azerbaijan and Ardabil provinces. Iran J Agric Sci 39:281–289

Golian S, Saghafian B, Sheshangosht S, Ghalkhani H (2010) Comparison of classification and clustering methods in spatial rainfall pattern recognition at Northern Iran. Theor Appl Climatol 102(3–4):319–329

Hamed KH (2008) Trend detection in hydrologic data: the Mann–Kendall trend test under the scaling hypothesis. J Hydrol 349:350–363

Hargreaves GH, Samani ZA (1985) Reference crop evapotranspiration from temperature. Appl Eng Agric 1(2):96–99

Heathcote RL (1986) The arid lands: their use and abuse. Longman, New York

Hulme M (1996) Recent climatic change in the world's drylands. Geophys Res Lett 23:61–64

IPCC (2007) In: Solomon S, Qin D, Manning M, Chen Z, Marquis M, Averyt KB, Tignor M, Miller HL (eds) Climate change 2007. The physical science basis. Contribution of Working Group I to the Fourth Assessment Report of the Intergovernmental Panel on Climate Change. Cambridge University Press, Cambridge, p 996

Jensen ME, Burman RD, Allen RG (eds) (1990) Evapotranspiration and irrigation water requirements. ASCE Manual 70, New York, 332 pp

Jhajharia D, Shrivastava SK, Sarkar D, Sarkar S (2009) Temporal characteristics of pan evaporation trends under the humid conditions of northeast India. Agric For Meteorol 149:763–770

Kampata JM, Parida BP, Moalafhi DB (2008) Trend analysis of rainfall in the headstreams of the Zambezi River Basin in Zambia. Phys Chem Earth 33:621–625

Karimi Kakhk M, Sepehri A (2011) Climate change trends during two periods in Hamedan and Tabriz. Water Soil Sci 20.1(4):143–156 (in Persian)

Khalili D, Farnoud T, Jamshidi H, Kamgar-Haghighi AA, Zand-Parsa Sh (2011) Comparability analyses of the SPI and RDI meteorological drought indices in different climatic zones. Water Resour Manag 25:1737–1757

Kohler MA (1949) Double-mass analysis for testing the consistency of records and for making adjustments. Bull Am Meteorol Soc 30:188–189

Kousari MR, Ekhtesasi MR, Tazeh M, Saremi Naeini MA, Asadi Zarch MA (2011) An investigation of the Iranian climatic changes by considering the precipitation, temperature, and relative humidity parameters. Theor Appl Climatol 103(3–4):321–335

Kumar S, Merwade V, Kam J, Thurner K (2009) Streamflow trends in Indiana: effects of long term persistence, precipitation and subsurface drains. J Hydrol 374(1–2):171–183

Le Houérou HN (1996) Climate change, drought and desertification. J Arid Environ 34:133–185

Liang L, Li L, Liu Q (2010) Temporal variation of reference evapotranspiration during 1961–2005 in the Taoer River basin of Northeast China. Agric For Meteorol 150:298–306

Liu Q, Yang Z, Cui B (2008) Spatial and temporal variability of annual precipitation during 1961–2006 in Yellow River Basin China. J Hydrol 361:330–338

Mohsin T, Gough WA (2009) Trend analysis of long-term temperature time series in the Greater Toronto Area (GTA). Theor Appl Climatol 101:311–327

Novotny EV, Stefan HG (2007) Stream flow in Minnesota: indicator of climate change. J Hydrol 334(3–4):319–333

Onder D, Aydin M, Berberoglu S, Onder S, Yano T (2009) The use of aridity index to assess implications of climatic change for land cover in Turkey. Turk J Agric For 33:305–314

Paltineanu C, Mihailescu IF, Seceleanu I, Dragota C, Vasenciuc F (2007) Using aridity indices to describe some climate and soil features in Eastern Europe: a Romanian case study. Theor Appl Climatol 90:263–274

Partal T, Kahya E (2006) Trend analysis in Turkish precipitation data. Hydrol Process 20:2011–2026

Penman HC (1948) Natural evaporation from open water, bare soil and grass. Royal Society of London Series A, pp 120–146

Rai RK, Upadhyay A, Ojha CSP (2010) Temporal variability of climatic parameters of Yamuna River Basin: spatial analysis of persistence, trend and periodicity. Open Hydrol J 4:184–210

Rebetez M, Reinhard M (2008) Monthly air temperature trends in Switzerland 1901–2000 and 1975–2004. Theor Appl Climatol 91:27–34

Sadeghi AR, Kamgar-Haghighi AA, Sepaskhah AR, Khalili D, Zand-Parsa Sh (2002) Regional classification for dryland agriculture in southern Iran. J Arid Environ 50:333–341

Sen PK (1968) Estimates of the regression coefficient based on Kendall's tau. J Am Stat Assoc 63:1379–1389

Tabari H, Aghajanloo M-B (2012) Temporal pattern of monthly aridity index in Iran with considering precipitation and evapotranspiration trends. Int J Climatol. doi:10.1002/joc.3432

Tabari H, Hosseinzadeh Talaee P (2011a) Analysis of trends in temperature data in arid and semi-arid regions of Iran. Glob Planet Chang 79:1–10

Tabari H, Hosseinzadeh Talaee P (2011b) Recent trends of mean maximum and minimum air temperatures in the western half of Iran. Meteorog Atmos Phys 111:121–131. doi:10.1007/s00703-011-0125-0

Tabari H, Hosseinzadeh Talaee P (2011c) Temporal variability of precipitation over Iran: 1966–2005. J Hydrol 396:313–320

Tabari H, Marofi S (2011) Changes of pan evaporation in the west of Iran. Water Resour Manag 25:97–111

Tabari H, Aeini A, Hosseinzadeh Talaee P, Shifteh Some'e B (2011a) Spatial distribution and temporal variation of reference evapotranspiration in arid and semi-arid regions of Iran. Hydrol Process 26:500–512. doi:10.1002/hyp. 8146

Tabari H, Marofi S, Ahmadi M (2011b) Long-term variations of water quality parameters in the Maroon River, Iran. Environ Monit Assess 177:273–287

Tabari H, Marofi S, Aeini A, Hosseinzadeh Talaee P, Mohammadi K (2011c) Trend analysis of reference evapotranspiration in the western half of Iran. Agric For Meteorol 151:128–136

Tabari H, Shifteh Somee B, Rezaian Zadeh M (2011e) Testing for long-term trends in climatic variables in Iran. Atmos Res 100:132–140

Tabari H, Abghani H, Hosseinzadeh Talaee P (2012a) Temporal trends and spatial characteristics of drought and rainfall in arid and semi-arid regions of Iran. Hydrol Process. doi:10.1002/hyp.8460

Tabari H, Hosseinzadeh Talaee P, Ezani A, Shifteh Some'e B (2012b) Shift changes and monotonic trends in autocorrelated temperature series over Iran. Theor Appl Climatol. doi:10.1007/s00704-011-0568-8

Tabari H, Nikbakht J, Shifteh Some'e B (2011d) Investigation of groundwater level fluctuations in the north of Iran. Environ Earth Sci. doi:10.1007/s12665-011-1229-z

Tabari H, Nikbakht J, Hosseinzadeh Talaee P (2012c) Identification of trend in reference evapotranspiration series with serial dependence in Iran. Water Resour Manag. doi:10.1007/s11269-012-0011-7

Theil H (1950) A rank invariant method of linear and polynomial regression analysis, part 3. Netherlands Akademie van Wettenschappen Proceedings 53:1397–1412

Thornthwaite CW (1948) An approach toward a rational classification of climate. Geogr Rev 38:55–94

Turkes M (1999) Vulnerability of Turkey to desertification with respect to precipitation and aridity conditions. Turk J Eng Environ Sci 23:363–380

Turkes M (2003) Spatial and temporal variations in precipitation and aridity index series of Turkey. In: Bölle H-J (ed) Mediterranean climate: variability and trends. Springer, Berlin, pp 181–213

UNEP (1992) World atlas of desertification. Edward Arnold, London

UNESCO (1979) Map of the world distribution of arid regions: Explanatory note. MAP Technical Notes 7. UNESCO, Paris, 54 pp + map

UNFCCC (2007) Climate change: impacts, vulnerabilities and adaptation in developing countries. United Nations Framework Convention on Climate Change

von Storch H, Navarra A (1995) Analysis of climate variability—applications of statistical techniques. Springer, New York

Wu SH, Yin Y, Zheng D, Yang Q (2006) Moisture conditions and climate trends in China during the period 1971–2000. Int J Climatol 26:193–206

Wu H, Soh LK, Samal A, Chen XH (2008) Trend analysis of streamflow drought events in Nebraska. Water Resour Manag 22:145–164. doi:10.1007/s11269-006-9148-6

Yue S, Hashino M (2003) Temperature trends in Japan: 1900–1996. Theor Appl Climatol 75:15–27

Yue S, Wang CY (2002) Applicability of prewhitening to eliminate the influence of serial correlation on the Mann–Kendall test. Water Resour Manag 38(6):1068. doi:10.1029/2001WR000861

Yue S, Pilon P, Phinney R, Cavadias G (2002) The influence of autocorrelation on the ability to detect trend in hydrological series. Hydrol Process 16:1807–1829. doi:10.1002/hyp. 1095

Yue S, Pilon P, Phinney R (2003) Canadian streamflow trend detection: impact of serial and cross-correlation. Hydrol Sci J 48(1):51–63

Zhang Q, Xu Ch-Y, Zhang Z (2009) Observed changes of drought/wetness episodes in the Pearl River basin, China, using the standardized precipitation index and aridity index. Theor Appl Climatol 98(1–2):89–99